


## NANO EXPRESS

## Open Access



# In Situ SR-XPS Observation of Ni-Assisted Low-Temperature Formation of Epitaxial Graphene on 3C-SiC/Si

Mika Hasegawa<sup>1\*</sup> , Kenta Sugawara<sup>1</sup>, Ryota Suto<sup>1</sup>, Shota Sambonsuge<sup>1</sup>, Yuden Teraoka<sup>2</sup>, Akitaka Yoshigoe<sup>2</sup>, Sergey Filimonov<sup>3</sup>, Hirokazu Fukidome<sup>1</sup> and Maki Suemitsu<sup>1,4</sup>

## Abstract

Low-temperature (~1073 K) formation of graphene was performed on Si substrates by using an ultrathin (2 nm) Ni layer deposited on a 3C-SiC thin film heteroepitaxially grown on a Si substrate. Angle-resolved, synchrotron-radiation X-ray photoemission spectroscopy (SR-XPS) results show that the stacking order is, from the surface to the bulk, Ni carbides ( $\text{Ni}_3\text{C}/\text{NiC}_x$ )/graphene/Ni/Ni silicides ( $\text{Ni}_2\text{Si}/\text{NiSi}$ )/3C-SiC/Si. In situ SR-XPS during the graphitization annealing clarified that graphene is formed during the cooling stage. We conclude that Ni silicide and Ni carbide formation play an essential role in the formation of graphene.

**Keywords:** Graphene, AR-XPS, 3C-SiC, Ni silicide, Ni carbide

## Background

Graphene, a single layer of  $\text{sp}^2$ -bonded carbon atoms arranged in a honeycomb lattice, has attracted much attention as a promising material in electronics and photonics. This is mainly due to its giant carrier mobility ( $200,000 \text{ cm}^2/\text{Vs}$ ) [1], high thermal conductivity, and high mechanical strength [2–4], as well as to its adaptability in integrated planar technology. Various methods of the graphene formation have been reported, including mechanical exfoliation of graphite [1], CVD on catalytic metals [5–8], and epitaxial graphene formation (EG) on hexagonal (4H- and 6H-) SiC bulk wafers [9–11]. Among these proposed methods, the EG method is considered preferable in that it not only allows growth of large-area graphene but also yields a well-defined graphene/substrate interface. This is because the method consists entirely of conventional thermal processes and is thus free from transfer of graphene onto substrates, unlike mechanical exfoliation and CVD methods, which sometimes causes the onset of wrinkles in graphene and residual impurities at the interface. The challenge of the EG method, however, is the cost of high-quality SiC bulk wafers and the use of

the SiC wafer itself, which forms a barrier for graphene to be adapted into Si technology.

In this context, Suemitsu et al. developed a so-called graphene-on-silicon (GOS) technology, in which EG is formed on a 3C-SiC thin film heteroepitaxially grown on a Si wafer [12–15]. The merit of the GOS method lies, first of all, in the use of large-area, cost-effective Si wafers, which makes this technology even more practical in Si technology. Moreover, GOS provides a good control over the structure of the graphene/SiC interface by simply changing the crystallographic orientation of the Si surface [16–18]. This allows to deliberately include or exclude the buffer layer at the graphene/SiC interface and thereby to control the electronic and optical properties of graphene as well. Several reports on the device fabrication based on GOS already exist [19–23].

A graphitization temperature of ~1473 K or higher, however, is still too high to be fully compatible with Si technology. Several attempts have been made to reduce the graphitization temperature of GOS, including the addition of a small amount of oxygen [24] or monosilane [25] into the vacuum used for the graphitization annealing. Although these methods succeeded in forming epitaxial graphene at ~1273 K, the graphene quality was much lower than that of the conventional GOS and EG methods. Recently, low-temperature (~973 K) formation of EG on

\* Correspondence: [mh7389@iec.tohoku.ac.jp](mailto:mh7389@iec.tohoku.ac.jp)

<sup>1</sup>Research Institute of Electrical Communications, Tohoku University, Sendai 980-8577, Japan

Full list of author information is available at the end of the article

SiC bulk crystals has been reported by Escobedo-Cousin et al. [26], who utilized a solid-phase chemical reaction between SiC and Ni. In fact, the formation of a “thin graphite layer” at low temperatures had been reported for ohmic-contact fabrication on SiC using Ni, well before [27] or at around the same time [28] of the rise of the graphene fever in the mid-2000s. Although these earlier studies suggested nickel silicide formation at the Ni/SiC interface and subsequent emission of excessive C atoms as a possible mechanism of the graphite formation, little is known about the details of the process. It has also been unclear whether this method is applicable to the GOS process, i.e., on 3C-SiC films. Here, we report the first application of this Ni-assisted graphene formation to GOS. Moreover, solid-phase reactions during heating/annealing/cooling procedures have been investigated in detail by using in situ synchrotron-radiation X-ray photoelectron spectroscopy (SR-XPS). Angle-resolved (AR) analysis was also utilized to clarify the stacking order of the layers. As a result, we demonstrate that this Ni-assisted method is equally applicable to 3C-SiC thin films (GOS), where graphene forms at temperatures less than 1273 K. We also clarify the role of Ni/SiC reactions, in which not only the formation of Ni silicide but also Ni carbonization is suggested as a key process in the formation of graphene.

## Methods

An n-type Si(111) wafer was cut into pieces to form specimens with a size of  $7 \times 7 \text{ mm}^2$ . The sample fabrication consists of four stages: (a) growth of 3C-SiC thin ( $\sim 100 \text{ nm}$ ) films using gas-source molecular-beam epitaxy (GSMBE), (b) ultrathin ( $\sim 2\text{--}3 \text{ nm}$ ) Ni film deposition using electron beam, (c) annealing at temperatures 973–1173 K for 30 min, and (d) cooling down to 373 K at a rate of 12.5 K/min. In GSMBE, monomethylsilane (MMS:  $\text{CH}_3\text{SiH}_3$ ) with a pressure of  $10^{-2} \text{ Pa}$  was used as the single source of silicon and carbon with a typical substrate temperature of 1323 K [29]. Graphitization annealing was conducted in ultrahigh vacuum (UHV) by heating the samples radiatively from the back with a graphite heater. Graphene formation was confirmed by Raman scattering spectroscopy. As for the analysis on reactions at the Ni/3C-SiC interface during heating/annealing/cooling of the samples, in situ SR-XPS observations were conducted at the BL23SU surface chemistry end-station [30] in the SPring-8 facilities using 650 eV photons. Angle-resolved (AR) observations were also conducted to obtain information on the order of the stacking layers. Since the photoelectrons that escape the surface at angles in the range of  $\pm 8^\circ$  around the line-of-sight direction from the surface to the analyzer were integrally collected in the present AR-XPS, only relative intensities between components were utilized in the analysis to avoid complexity.

## Results and Discussion

### Confirmation of Graphene Formation

Figure 1 shows the Raman spectra of the samples after annealing at three different temperatures. At temperatures 1073 and 1173 K, the three major fundamental vibration modes of graphene, i.e., G ( $\sim 1600 \text{ cm}^{-1}$ ), G' ( $\sim 2700 \text{ cm}^{-1}$ ), and D ( $\sim 1360 \text{ cm}^{-1}$ ) appear, which proves the graphene formation at these low temperatures. The grain size of graphene ( $L_a$ ) is obtained from the intensity ratio between the D and G bands as

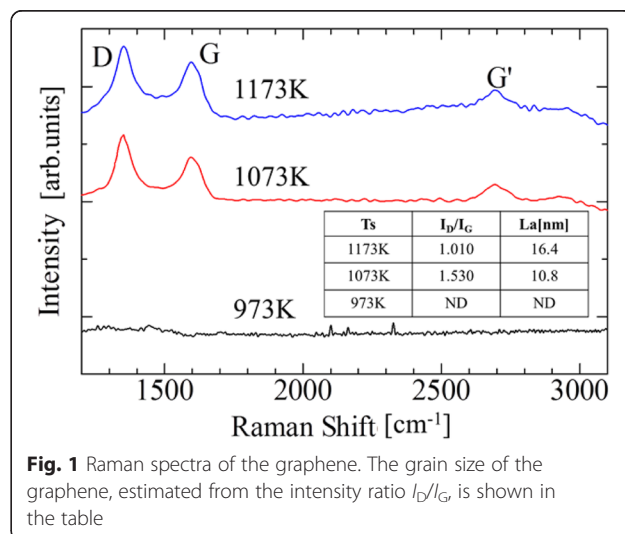
$$L_a(\text{nm}) = \frac{560}{E_{\text{laser}}^4} \left( \frac{I_D}{I_G} \right)^{-1},$$

where  $E_{\text{laser}}$  is the energy of the excitation laser in electron volt, and  $I_D$  and  $I_G$  are the intensities of the D and G bands, respectively [31]. At 1173 K, the estimated grain size is larger than that at 1073 K, as shown in the inset of Fig. 1.

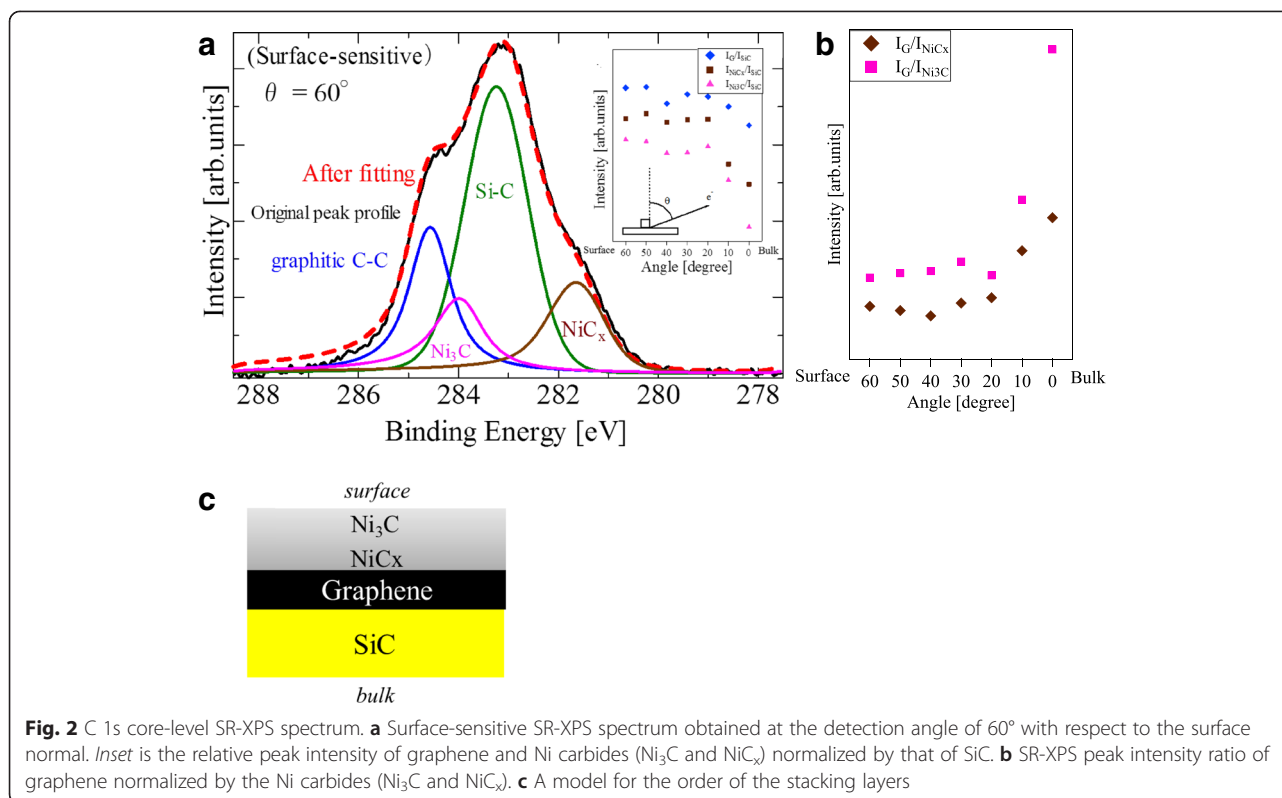
### The Mechanism of Ni-Assisted Graphene Formation

#### Determination of the Stacking Order of the Layers

Where is the graphene in the multi-layered Ni/SiC/Si structure? To answer this question, we conducted an AR-XPS analysis. Figure 2a shows the C 1s core-level spectrum obtained in a surface-sensitive mode with the detection angle of  $60^\circ$  from the surface normal. The Ni carbide components such as  $\text{Ni}_3\text{C}$  ( $\sim 284 \text{ eV}$ ) and  $\text{NiC}_x$  ( $\sim 282 \text{ eV}$ ,  $x > 0.33$ ) [32] appear in the spectrum together with the ones from 3C-SiC ( $\sim 283.5 \text{ eV}$ ) and graphene ( $\sim 284.5 \text{ eV}$ ) [33]. The escape depths  $\lambda$  of the photoelectrons from Ni-C, Ni, and Ni-Si layers are in the order of 1–1.7 nm, which decreases down to 0.5–0.8 nm in the surface-sensitive measurement at  $\theta = 60^\circ$ . Although this value is less than the thickness of the Ni layer ( $\sim 2 \text{ nm}$ ), we here observe a strong SiC component in the C 1s



**Fig. 1** Raman spectra of the graphene. The grain size of the graphene, estimated from the intensity ratio  $I_D/I_G$ , is shown in the table

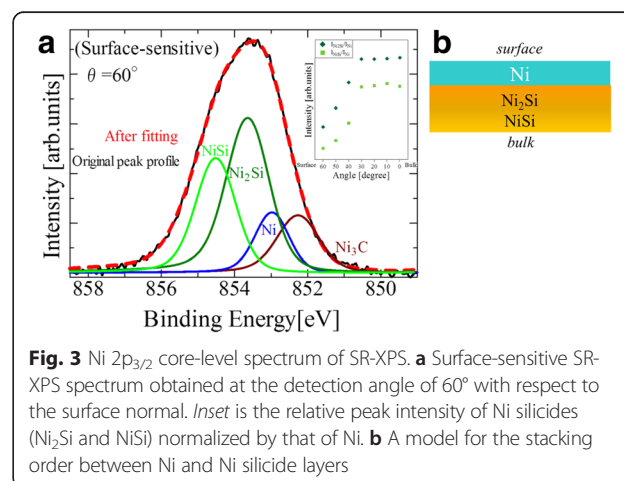


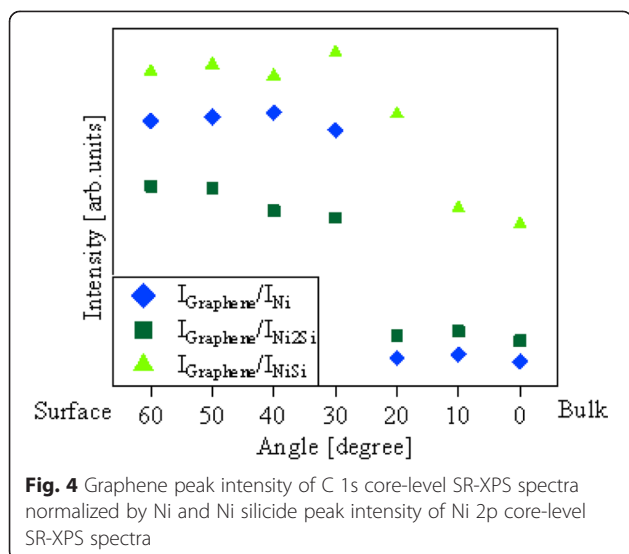
spectrum. This result can be related to the fact (a) that XPS measurement substantially detects photoelectrons from the surface up to  $3\lambda$  in depth and (b) that our XPS setup integrally collects the photoelectrons that leave the surface at angles in the range of  $\pm 8^\circ$  around the line-of-sight direction from the surface to the analyzer. The inset shows the detection-angle dependence of the peak intensities normalized by that of the SiC peak. The graphene and the Ni-carbide peaks show higher intensities in the surface-sensitive observations, indicating the formation of these layers on top of the SiC film. Figure 2b shows the relative peak intensity of graphene against  $\text{Ni}_3\text{C}$  and  $\text{NiC}_x$ . They are higher in the bulk-sensitive observations, and this tendency is pronounced in the  $I_G/I_{\text{Ni}_3\text{C}}$  ratio. It is therefore concluded that the graphene layer is located beneath the Ni carbide layers, and the  $\text{Ni}_3\text{C}$  layer is located above the C-rich  $\text{NiC}_x$  ( $x > 0.33$ ) layer (Fig. 2c).

Figure 3a shows the Ni  $2p_{3/2}$  core-level spectrum obtained in a surface-sensitive mode with the detection angle of  $60^\circ$  from the surface normal. The Ni silicide components such as  $\text{Ni}_2\text{Si}$  ( $\sim 854$  eV) and  $\text{NiSi}$  ( $\sim 854.9$  eV) and the Ni carbide component  $\text{Ni}_3\text{C}$  (852.4 eV) [34] appear in the spectrum as well as the one from Ni ( $\sim 853$  eV). The inset shows the detection-angle dependence of the Ni silicide peak intensities normalized to that of the Ni peak. They show higher intensities in the bulk-sensitive observations, indicating that the Ni silicides are located beneath the Ni layer. It is also noted that the relative intensity of

$\text{Ni}_2\text{Si}$  to  $\text{NiSi}$  increases in the surface-sensitive observations, indicating that the Ni-rich  $\text{Ni}_2\text{Si}$  silicide is on top of the Si-rich  $\text{NiSi}$  silicide. We therefore conclude that the Ni and Ni-silicide layers are stacked, from the surface to the bulk, in the order of Ni/ $\text{Ni}_2\text{Si}$ / $\text{NiSi}$  (Fig. 3b).

Figure 4 shows the detection-angle dependence of the relative intensity of the graphene peak normalized by that of Ni and Ni silicides. It shows higher intensities in the surface-sensitive observations. It is thus concluded that graphene is formed on top of the Ni and Ni silicide films. The inflection points seen at  $20$ – $30^\circ$  are currently related to a possible abruptness at interfaces, but its



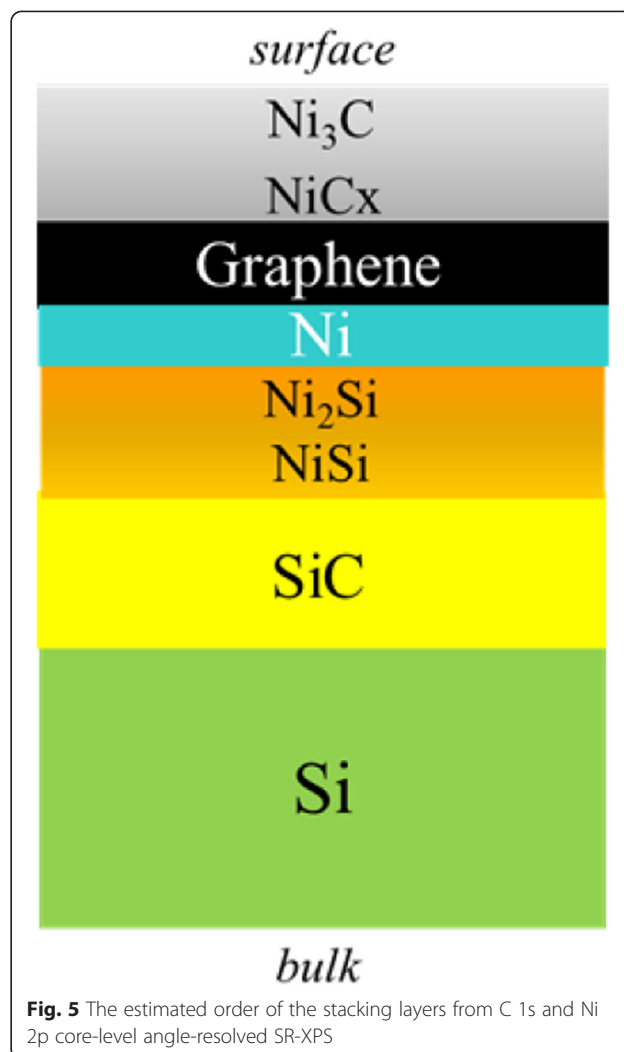


detailed understandings are open to future studies. By summing up all the AR-XPS results, we conclude that the order of the stacking is as shown in Fig. 5.

#### *In Situ SR-XPS Observation of the Graphene Formation*

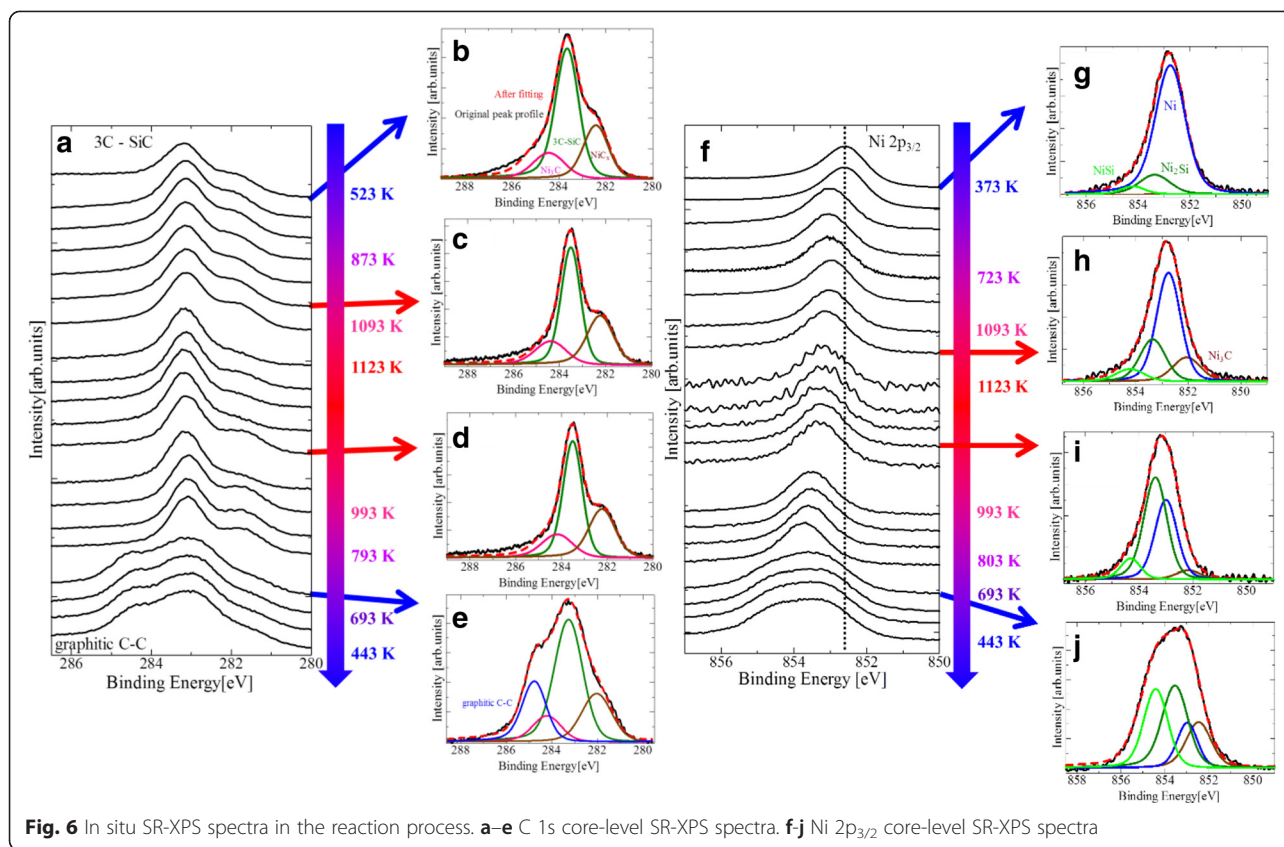
In order to clarify the role of reactions between Ni and SiC on the formation of graphene, in situ SR-XPS was conducted during heating, annealing (1123 K for 30 min), and cooling of the sample (Fig. 6a). The Ni carbide components, Ni<sub>3</sub>C and NiC<sub>x</sub> as well as that of 3C-SiC, appear in the spectra in the early stage of the heating. Graphene component, on the other hand, appears only in the cooling stage (Fig. 6e). In the Ni 2p<sub>3/2</sub> core-level SR-XPS spectra (Fig. 6f), the peak shifts to higher binding energies during the heating/annealing procedures. This blue shift could mean either formation of Ni silicides [34] or Ni carbides [35], or both, and is shown to be accelerated during the cooling stage. Specifically, the Ni-rich silicide Ni<sub>2</sub>Si first forms during heating and NiSi and Ni<sub>3</sub>C form during annealing and cooling.

From these time evolutions of both C 1s and Ni 2p core-level peaks, we conclude that part of the 3C-SiC film is decomposed due to reactions with Ni to form Ni silicides and Ni carbides, and the excess C atoms created by this decomposition are used to form graphene. Of the Ni silicide and carbide formations, the former should be by far the major reaction path because the formation enthalpy for Ni silicide is negative (−80 kJ/mol) while that for Ni carbide is positive (30 kJ/mol) [35–37]. Kurimoto et al. [27] also suggested Si diffusion into the Ni layer to form Ni<sub>2</sub>Si as a major reaction path for the graphite layer formation. As for graphene, Cao et al. [28] have reported the formation of an amorphous C layer followed by its constituents diffusing toward the surface as a possible mechanism. A new finding in this study, however, is that



part of the excess C atoms is used for the formation of Ni carbides as well, as shown in Figs. 2 and 6. Since the formation of Ni carbide is prohibited at normal pressures for our annealing temperatures [36, 38], the present observation of Ni carbide should be related to the fact that our annealing was conducted under a non-equilibrium UHV condition, unlike the ohmic-contact fabrication process conducted at normal pressures. In any case, the rest of the C atoms are dissolved in Ni as a result of the high solubility (~2.7 %) in Ni at high temperatures (>1000 K). Upon cooling, these dissolved C atoms are prone to segregate to the surface to decrease the surface energy [39, 40]. In the present case, however, the surface of Ni is already covered with Ni carbide layers, whose solubility for C atoms is too low (~0.01 %) [41] either to accommodate them therein or to let them diffuse through the layer to the surface. This is understood to be the reason why excess C atoms take the form of graphene at the interface between Ni and Ni carbides.





## Conclusions

In order to verify the Ni-assisted graphene formation on the SiC thin films on Si substrates and to clarify its growth mechanism, we conducted Raman and in situ SR-XPS analysis. We have successfully demonstrated that graphene actually forms on a 3C-SiC thin film at a temperature as low as 1073 K with the aid of the Ni layer. Angle-resolved SR-XPS proved that the stacking order, from the top to the bottom, is Ni carbides (Ni<sub>3</sub>C/NiC<sub>x</sub>)/graphene/Ni/Ni silicides (Ni<sub>2</sub>Si/NiSi)/SiC/Si. In situ SR-XPS during heating/annealing/cooling procedures has proved that Ni silicides and Ni carbides form during heating/annealing periods while graphene forms only in the cooling period. It is suggested that excess C atoms are liberated during heating/annealing along with the formation of Ni silicides, and part of these excess C atoms form into graphene. Graphene is formed during cooling because the C atom solubility in Ni decreases with decreasing temperature. The Ni carbide layers are suggested to act as a good capping layer for graphene formation as well as a C source through its decomposition during cooling, which is favored because of its exothermic nature of the reaction.

The obtained graphene quality is still mediocre (D/G Raman ratio ~1.0), and there is a lot of room for improvement toward low-temperature formation of graphene. Moreover, graphene produced by this method grows on a

non-crystalline Ni layer, not directly on the SiC crystal, which cannot be called “epitaxial graphene” in its true meaning of the term. Despite these limitations, the present findings, especially that on the role of Ni carbide formation, will greatly contribute to the improvement of Ni-assisted graphene formation on Ni/SiC as well as ohmic-contact formation for both graphene and SiC devices.

## Competing Interests

The authors declare that they have no competing interests.

## Authors' Contributions

MH contributed extensively to the work presented in this paper and wrote the paper. KS and SS designed and performed Raman experiments. RS, YT, and AY performed SR-XPS and AR-XPS. SF led the discussion on the role of Ni silicidation and carbonization. HF analyzed the data of AR-XPS. MS designed the overall project including details of the experiment and led the discussion together with SF. All authors read and approved the final manuscript.

## Acknowledgements

The synchrotron radiation experiments were performed at BL23SU of SPring-8 with the approval of the Japan Synchrotron Radiation Research Institute (JASRI) and Japan Atomic Energy Agency (JAEA), supported by Mext Nanotechnology Network Program and Mext Nanotechnology Platform Japan Program (Proposal No. 2012A3807, 2012B3807, and 2013B3875). Part of this work was supported by *Kakenhi* (23000008, 25286053, 25600091). The authors thank Karsten Horn for a careful reading of the manuscript.

## Author details

<sup>1</sup>Research Institute of Electrical Communications, Tohoku University, Sendai 980-8577, Japan. <sup>2</sup>JAEA, Kouto, Sayo-cho, Sayo-gun, Hyogo 679-5148, Japan.

<sup>3</sup>Department of Physics, Tomsk State University, Tomsk, Russia. <sup>4</sup>JST-CREST, Tokyo, Chiyoda, Tokyo 107-0075, Japan.

Received: 2 September 2015 Accepted: 19 October 2015

Published online: 26 October 2015

## References

- Novoseliv KS, Geim AK, Morozov SV, Jiang D, Dubonos SV, Grigorieva IV, Firsov AA (2004) Electric field effect in atomically thin carbon films. *Science* 306:666
- Lee C, Wei X, Kysar JW, Hone J (2008) Measurement of the elastic properties and intrinsic strength of monolayer graphene. *Science* 18:385
- Castro Neto AH, Guinea F, Peres NMR, Novoselov KS, Geim AK (2009) The electronic properties of graphene. *Rev Mod Phys* 81:109
- Kadzierski J, Hsu PL, Healey P, Wyatt PW, Keast CL, Sprinkle M, Berger C, de Heer WA (2007) Epitaxial graphene transistors on SiC substrates. *IEEE Trans Electron Devices* 55:2008
- Trombros N, Jozsa C, Popinciuc M, Jonkman HT, van Wees BJ (2007) Electronic spin transport and spin precession in single graphene layers at room temperature. *Nature* 448:571
- Sutter PW, Flege J, Sutter EA (2009) Epitaxial graphene on ruthenium. *Nat Mater* 7:406
- Kim KS, Zhao Y, Jang H, Lee SY, Kim JM, Kim KS, Ahn J-HA, Kim P, Choi J-Y, Hong H (2009) Large-scale pattern growth of graphene films for stretchable transparent electrodes. *Nature* 457:706
- Kondo D, Sato S, Yagi K, Harada N, Sato M, Nihei M, Yokoyama N (2010) Low-temperature synthesis of graphene and fabrication of top-gated field effect transistors without using transfer processes. *Appl Phys Express* 3:025102
- Forbeaux I, Themlin JM, Debever JM (1998) Heteroepitaxial graphite on 6H-SiC(0001): interface formation through conduction-band electronic structure. *Phys Rev B: Condens Matter Mater Phys* 58:16396
- Berger C, Song Z, Li X, Wu X, Brown N, Naud C, Mayou D, Li T, Hass J, Marchenkov AN, Conrad EH, First PN, de Heer WA (2006) Electronic confinement and coherence in patterned epitaxial graphene. *Science* 312:1191
- Ernstev KV, Bostwick A, Horn K, Jobst J, Kellogg GL, Ley L, MaChesney JL, Ohta T, Reshanov SA, Rohrl J, Rotenberg E, Schmid AK, Waldmann D, Weber HB, Seyller T (2009) Towards wafer-size graphene layers by atmospheric pressure graphitization of silicon carbide. *Nat Mater* 8:203
- Suemitsu M, Miyamoto Y, Handa H, Konno A (2009) Graphene Formation on a 3C-SiC(111) thin film grown on Si(110) substrates. *e-J Surf Sci Nanotechnol* 7:311
- Miyamoto Y, Handa H, Saito E, Konno A, Narita Y, Suemitsu M, Fukidome H, Ito T, Yasui K, Nakazawa H, Endoh T (2009) Raman-scattering spectroscopy of epitaxial graphene formed on SiC film on Si substrate. *e-J Surf Sci Nanotechnol* 7:107
- Fukidome H, Miyamoto Y, Handa H, Saito E, Suemitsu M (2010) Epitaxial growth processes of graphene on silicon substrates. *Jpn J Appl Phys* 49:01AH03
- Fukidome H, Takahashi R, Miyamoto Y, Handa H, Kang HC, Karasawa H, Suemitsu T, Otsuji T, Yoshigoe A, Teraoka Y, Suemitsu M (2010) Epitaxial graphene on silicon toward graphene-silicon fusion electronics. *arXiv*. 1001:4955
- Suemitsu M, Fukidome H (2010) Epitaxial graphene on silicon substrates. *J Phys D43:374012*
- Handa H, Takahashi R, Abe S, Imaizumi K, Saito E, Jung M-H, Ito S, Fukidome H, Suemitsu M (2011) Transmission electron micro Raman-scattering spectroscopy observation on the interface structure of graphene formed on Si substrates with various orientations. *Jpn J Appl Phys* 50:04DH02
- Takahashi R, Handa H, Abe S, Imaizumi K, Fukidome H, Yoshigoe A, Teraoka Y, Suemitsu M (2011) Low-energy-electron-diffraction and x-ray-phototelectron -spectroscopy studies of graphitization of 3C-SiC(111) thin film on Si(111) substrate. *Jpn J Appl Phys* 50(7):70103-1-70103-6
- Moutaouakil AE, Kang H, Handa H, Fukidome H, Suemitsu T, Sano E, Suemitsu M, Otsuji T (2011) Room temperature logic inverter on epitaxial graphene-on-silicon device. *Jpn J Appl Phys* 50(7):70113-1-70113-4
- Kang H-C, Olac-vaw R, Karasawa H, Miyamoto Y, Handa H, Suemitsu T, Fukidome H, Suemitsu M, Otsuji T (2010) Extraction of drain current and effective mobility in epitaxial graphene channel field-effect transistors on SiC layer grown on silicon substrates. *Jpn J Appl Phys* 49:04DF17
- Olac-vaw R, Kang H-C, Karasawa H, Miyamoto Y, Handa H, Fukidome H, Suemitsu T, Suemitsu M, Otsuji T (2010) Ambipolar behavior in epitaxial graphene-based field-effect transistors on Si substrate. *Jpn J Appl Phys* 49:06GG01
- Kang H-C, Karasawa H, Miyamoto Y, Handa H, Fukidome H, Suemitsu T, Suemitsu M, Otsuji T (2010) Epitaxial graphene top-gate FETs on silicon substrates. *Solid-State Electron* 54:1071-1075
- Suemitsu T, Kubo M, Handa H, Takahashi R, Fukidome H, Suemitsu M, Otsuji T (2011) Graphene/SiC/Si FETs with SiCN gate stack. *ECS Trans* 41(6):249
- Imaizumi K, Handa H, Takahashi R, Saito E, Fukidome H, Enta Y, Teraoka Y, Yoshigoe A, Suemitsu M (2011) Oxygen-induced reduction of the graphitization temperature of SiC surface. *Jpn J Appl Phys* 50:70105
- Sanbonsuge S, Abe S, Handa H, Takahashi R, Imaizumi K, Fukidome H, Suemitsu M (2012) Improvement in film quality of epitaxial graphene on SiC(111)/Si(111) by SiH4 pretreatment. *Jpn J Appl Phys* 51(6):06FD10-1-06FD10-4
- Escobedo-Cousin E, Vassilevski K, Hopf T, Wright N, O'Neill A, Horsfall A, Goss J, Cumpson P (2013) Optimising the growth of few-layer graphene on silicon carbide by nickel silicidation. *Mater Sci Forum* 740-742:121-124
- Kurimoto E, Harima H, Toda T, Sawada M, Nakashima S (2002) Raman study on the Ni/SiC interface reaction. *J Appl Phys* 91(12):10215-10217
- Cao Y, Nyborg L, Yi D-Q, Jelvestam U (2006) Study of reaction process on Ni/4H-SiC contact. *Mat Sci Technol* 22(10):1227-1234
- Fukidome H, Takahashi R, Abe S, Imaizumi K, Handa H, Kang H-C, Karasawa H, Suemitsu T, Otsuji T, Enta Y, Yoshigoe A, Teraoka Y, Kotsugi M, Ohkouchi T, Kinoshita T, Suemitsu M (2011) Control of epitaxy of graphene by crystallographic orientation of a Si substrate toward device applications. *J Mater Chem* 21:17242-17248
- Teraoka Y, Yoshigoe A (1999) Precise control of Si(001) initial oxidation by translational kinetic energy of O2 molecules. *Jpn J Appl Phys* 38(suppl 38-1):b42
- Pimenta MA, Dresselhaus G, Dresselhaus MS, Cancado LG, Jorio A, Saito R (2007) Studying disorder in graphite-based systems by Raman spectroscopy. *Phys Chem Chem Phys* 9:1276
- Czekaj I, Loviat F, Raimondi F, Wambach J, Biollaz S, Wokaun A (2007) Characterization of surface processes at the Ni-based catalyst during the methanation of biomass-derived synthesis gas: x-ray photoelectron spectroscopy (XPS). *Appl Catal Gen* 329:68-78
- Ernstev KV, Speck F, Seyller T, Riley JD, Ley L (2008) Interaction, growth, and ordering of epitaxial graphene on SiC{0001} surfaces: a comparative photoelectron spectroscopy study. *Phys Rev B* 77:15530
- Tam PL, Nyborg L (2009) Sputter deposition and XPS analysis of nickel silicide thin films. *Surf & Coating Technol* 203:2886-2890
- Narita K (1969) *J Japan Inst Metals* 8:49
- Chandrasekharaiah MS, Margrave JL, O'Hare PAG (1993) *J Phys Chem Ref Data* 22(6):1459-1468
- Cao Y, Nyborg L (2011) Properties and Applications of Silicon Carbide. pp 171-194 <http://www.intechopen.com/books/properties-and-applications-of-silicon-carbide/contact-formation-on-silicon-carbide-by-use-of-nickel-and-tantalum-in-a-materials-science-point-of-v>
- The Japan Institute of Metals: *The Metal Databook*. 530 2004
- Fujita D, Homma T (1992) Surface precipitation of graphite layers on carbon-doped nickel and their stabilization effect against chemisorption and initial oxidation. *Surf Interface Anal* 19:430-434
- Fujita D, Yoshihara K (1994) Surface precipitation process of epitaxially grown graphite (0001) layers on carbon-doped nickel(III) surface. *J Vac Sci Technol A* 12:2134-2139
- Fujita D (2003) Synthesis of new carbon nanostructures by surface precipitation -carbon nano-sprout-. *J Surf Anal* 10(3):218-229